

Self-Averaging in the Three Dimensional Site Diluted Heisenberg Model at the critical point

A. G. Ordillo-Guerrero and J. J. Ruiz-Lorenzo

Departamento de Física, Universidad de Extremadura, E-06071 Badajoz, Spain. and
Instituto de Biotecnología y Física de Sistemas Complejos (BIFI), Zaragoza, Spain.
(Dated: May 17, 2007)

We study the self-averaging properties of the three dimensional site diluted Heisenberg model. The Harris criterion [1] states that disorder is irrelevant since the specific heat critical exponent of the pure model is negative. According with some analytical approaches [2], this implies that the susceptibility should be self-averaging at the critical temperature ($R = 0$). We have checked this theoretical prediction for a large range of dilution (including strong dilution) at criticality and we have found that the introduction of scaling corrections is crucial in order to obtain self-averageness in this model. Finally we have computed critical exponents and cumulants which compare very well with those of the pure model supporting the Universality predicted by the Harris criterion.

PACS numbers: 75.50.-Lk, 05.50.+q, 68.35.Rh, 75.40.Cx

I. INTRODUCTION

It is a well known fact that a possible way to obtain new Universality classes is to add disorder to pure systems. The Harris criterion, Ref. [1], states that if the specific heat diverges in the pure system, the disorder will change the critical behavior of the model, i.e. a new Universality class will appear. Conversely, if the specific heat does not diverge in the pure system the critical exponents of the disordered system will not change.

The aim of this paper is to study the dependence of some observables with the disorder (self-averaging properties). The study of the self-averaging properties in disordered systems has generated in the past years a large amount of both analytical, see Refs. [2, 3, 4], and numerical, see Refs. [5, 6, 7], works. We will focus in the computation at criticality of the quantity R , which will be defined later and is a measure of the self-averageness of the susceptibility.

We will study the three dimensional site diluted Heisenberg model with quenched disorder (in which, according to Ref. [1], the disorder is irrelevant) in order to test the analytical predictions.

To obtain accurate measures of critical properties, in particular of R , we will use Finite Size Scaling (FSS) techniques as the quotient method [8, 9] that allow us to work in large lattices at the critical point and to perform in finite volume extrapolations.

We will show results strongly supporting that this R cumulant is zero at the critical point, but only taking into account the scaling corrections, against some theoretical predictions (Ref. [3]) and supporting others [2, 4].

The structure of the paper is as follows. In the next section we summarize some analytical predictions concerning the self-averaging properties of diluted models at criticality. In section III we define the model and the observables. In the first part of section IV we describe our simulation methods, in the second part we analyze deeply the correction to scaling exponent, ν , while in the last part we give our numerical results concerning self-

averaging properties of the susceptibility both in vector and tensor channels. Results related to the universality of the critical exponents and cumulants are given in Appendix A. Finally we give our conclusions in section V.

II. ANALYTICAL PREDICTIONS

The self-averaging (SA) of the susceptibility is defined in terms of:

$$R = \frac{\overline{M^2 i^2} - \overline{M^2} \overline{i^2}}{\overline{M^2 i^2}}; \quad (1)$$

being M the total magnetization. The susceptibility is self-averaging if $R \rightarrow 0$ as $L \rightarrow \infty$.

In Ref. [2], the following picture was found:

1. Outside the critical temperature: $R = 0$. Can be found, based in Renormalization Group (RG) or using general statistical arguments, that $R \propto (T - T_c)^{\nu}$ in a finite geometry, being L the system size and ξ the correlation length, which is finite for $T \neq T_c$: then $R \rightarrow 0$ as $L \rightarrow \infty$. This is called Strong SA.
2. At the critical temperature, a Renormalization Group analysis opens two possible scenarios:

Models in which according with the Harris criterion the disorder is relevant ($\nu_{\text{pure}} > 0$): $R \neq 0$. The susceptibility at the critical point is not self-averaging. In particular, Ref. [2] shows that in these conditions R is proportional to the fixed point value of the coupling which induces the disorder in the Hamiltonian, which controls the new Universality class. This is called no SA.

Models in which according with the Harris criterion the disorder is not relevant ($\nu_{\text{pure}} < 0$):

$R = 0$. The susceptibility at the critical point is self-averaging. In a finite geometry R scales as $L^{-\nu}$, where ν and β are the critical exponents of the pure system, which are the same in the disordered one. This is called Weak SA.

The observable R has been measured in other diluted models: for example in the four dimensional diluted Ising model, see Ref. [10]. In this model a Mean Field computation and a numerical one found a non zero value for R although the diluted model was shown to belong of the same universality class of the pure model, contradicting the conclusions of Ref. [2]. One can claim that the logarithms which live in the upper critical dimension do the numerical analysis difficult. In particular was found analytically in Mean Field $R = 0.31024$ and numerically $R = 0.315 \pm 0.032$. Because the logarithms, it was impossible to do an infinite volume extrapolation for the numerical values of R . Notice that in this model the only fixed point is the Gaussian one (all the values of the couplings are zero) and, following Ref. [2], R should be zero.

In addition a two-loops field theory calculation done in Ref. [3] predicts a non zero value for R for the diluted Heisenberg model (in which the disorder is irrelevant, $\nu_{\text{pure}} = 0.134$, see Ref. [11]). The two-loops field theoretical prediction for R in the pure case was $\nu_{\text{pure}} > 0$, so, apparently, this work is consistent with the findings of Ref. [2]. The starting point in Ref. [3] was the Mean Field computation done in Ref. [10], modifying it to take into account the vector degrees of freedom, introducing the fluctuations using the Brezin-Zinn-Justin (BZJ) method, Ref. [12]. They found analytically $R = 0.022688$ for the vector channel and universal (independent of the dilution for all $p < 1$). It is important to remark that in the BZJ method one goes from the beginning the temperature of the system to the infinite volume critical one working in a finite geometry, so in order to compute R in this scheme the following sequence of limits is used:

$$R = \lim_{L \rightarrow \infty} \lim_{T \rightarrow T_c} R(L; T); \quad (2)$$

where R is the infinite volume extrapolation at criticality of $R(L; T)$, and T_c is the infinite volume critical temperature of the system. The other possible limits sequence that can be computed is:

$$\lim_{T \rightarrow T_c} \lim_{L \rightarrow \infty} R(L; T); \quad (3)$$

which is zero even when the disorder is relevant since $R \propto L^{-d}$ as $T \rightarrow T_c$.

Hence, in order to test these discrepancies we have simulated numerically the site diluted three dimensional Heisenberg model computing R in the vector and tensor channels. To perform this program, in particular in doing the infinite volume extrapolations of cumulants and exponents, is really important a proper use of the corrections to scaling.

III. THE MODEL

The Heisenberg site-diluted model in three dimensions is defined in terms of $O(3)$ spin variables placed in the nodes of a cubic three-dimensional lattice, with Hamiltonian:

$$H = \sum_{\langle i,j \rangle} S_i \cdot S_j; \quad (4)$$

where the S_i are three-dimensional vectors of unity modulus, and the sum is extended only over nearest neighbors. The disorder is introduced by the random variables δ_i which take on value 1 with probability p and 0 with probability $1 - p$. An actual configuration, will be called a sample.

In addition, as done in Ref. [8], we define a tensorial channel associated with the vector S through the traceless tensor:

$$T_{ij} = S_i S_j - \frac{1}{3} \delta_{ij}; \quad i, j = 1, 2, 3; \quad (5)$$

In the following, we shall denote a thermal average with brackets, while the sample average will be overlined. The observables will be denoted with calligraphic letters, i.e. \mathcal{O} , and with italics the double average, $\mathcal{O} = \overline{\langle \mathcal{O} \rangle}$. We define the total nearest-neighbor energy as:

$$E = \sum_{\langle i,j \rangle} S_i \cdot S_j; \quad (6)$$

and the normalized magnetization for both channels as

$$M = \frac{1}{V} \sum_i S_i; \quad (7)$$

$$M_T = \frac{1}{V} \sum_i (S_i S_i - \frac{1}{N}); \quad (8)$$

being V the volume (defined as L^3 , where L is the lattice size). Because of the finite probability to reach every minimum value for the free energy, the thermal average of Eqs. (7) and (8), is zero in a finite lattice. Therefore, we have to define the order parameters as the $O(3)$ invariant scalars:

$$M = \overline{\langle M^2 \rangle}; \quad M_T = \overline{\langle M_T^2 \rangle}; \quad (9)$$

We also define both susceptibilities as:

$$\chi = V \overline{\langle M^2 \rangle}; \quad \chi_T = V \overline{\langle M_T^2 \rangle}; \quad (10)$$

A very useful quantity is the Binder parameter, defined as:

$$g_4^V = 1 - \frac{1}{3} \frac{\overline{\langle M^4 \rangle}}{\overline{\langle M^2 \rangle}^2}; \quad g_4^T = 1 - \frac{\overline{\langle M_T^4 \rangle}}{3 \overline{\langle M_T^2 \rangle}^2}; \quad (11)$$

Other kind of Binder parameter, meaningless for the pure system, can be defined as:

$$g_2^V = \frac{\overline{hM^2 i^2} \overline{hM^2 i^2}}{\overline{hM^2 i^2}^2}; \quad g_2^T = \frac{\overline{h(\text{tr} M^2_T) i^2} \overline{h(\text{tr} M^2_T) i^2}}{\overline{h(\text{tr} M^2_T) i^2}^2}; \quad (12)$$

these are the quantities we are using to estimate the self-averaging properties of the susceptibility (χ) in both channels.

A very convenient definition of the correlation length in a finite lattice reads, see Ref. [13]:

$$\xi = \frac{F}{4 \sin^2(\pi/L)}^{\frac{1}{2}}; \quad (13)$$

where F is defined in terms of the Fourier transform of the magnetization:

$$F(k) = \frac{1}{V} \sum_r e^{ik \cdot r} S_r \quad (14)$$

as:

$$F = \frac{V}{3} \overline{hF(2\pi/L; 0; 0)^2} + \text{permutations} i; \quad (15)$$

The same definition is also valid in the tensorial case. This definition is very well behaved for the finite-size scaling (FSS) method we have employed, see Ref. [8]. Finally, we measure the specific heat as:

$$C = V^{-1} \overline{hE^2 i} - \overline{hE i}^2; \quad (16)$$

IV. SIMULATIONS

A. Description

The lattice sizes L we have studied are 8;12;16;24;32;48;64, and, only in the pure model, $L = 96$.

Between each measure of the observables described in Sec. III, firstly, we update the spin-variables using a Metropolis method over a 10% of the individuals spins, chosen at random, then we perform a number (growing with L) of cluster updates using a Wolff method, see Ref. [14], this is our Elementary Monte Carlo Step (EMCS). The number of clusters traced (or Wolff updates) between measures have been chosen to yield a good value of the self-correlation time, see Ref. [14], in our case always $1 < \tau < 2$ (τ being the integrated autocorrelation time of the energy).

In order to work in thermally-equilibrated systems we perform a great number of EMCS. We start the simulation always from random (hot) distributions of the spin-variables, although we have checked out that averages do not change if we begin from cold configurations (i.e. all spins being in the same direction). To concrete, we have taken $4 \cdot 10^6$ measures for the pure model discarding

about 10^5 of the first measures for $L = 8$ and growing this number with the lattice size. We have performed $2 \cdot 10^4$ quenched disorder realizations in the diluted models independently of the dilution and the lattice size and taking 100 measures per sample, according to Ref. [10] who demonstrated that the best approach to minimize the statistical error is to simulate a great number of samples with a few measures in each one.

To measure the critical exponents, we use the so-called quotients method [8, 9], which allows for a great statistical accuracy. The starting point is the equation:

$$Q_0 \frac{Q}{Q_0} = s^{x_0} + O(L^{-1}); \quad (17)$$

With Q_0 being the quotient of the observable Q measured in a pair of lattices of sizes L and sL , at the temperature where $Q = s$, being 1 the eigenvalue corresponding to the first irrelevant operator on the language of the RG theory. We have fixed $s = 2$ in our case. Therefore, firstly we need to estimate by successive simulations the point where:

$$\frac{(2L; p)}{2L} = \frac{(L; p)}{L}; \quad (18)$$

for each pair of lattices $(L; 2L)$, then we have used re-weighting techniques to tune this condition. These re-weighting techniques are used to extrapolate the observables and calculate their derivatives, always before the sample-average is performed. The equations used are, see Refs. [10, 14]:

$$hO_i(p + \delta p) = hO_i(p) e^{\delta p \frac{\partial hO_i}{\partial p}}; \quad (19)$$

$$\frac{\partial hO_i}{\partial p} = \frac{\partial hO_i}{\partial p} = \frac{O_i E_i}{O_i E_i}; \quad (20)$$

These extrapolations are biased, for instance, the expectation value of Eq.(20), when the averages are calculated with N_m measures is:

$$\frac{1}{N_m} \sum_{i=1}^{N_m} \frac{\partial hO_i}{\partial p}; \quad (21)$$

hence, we have to correct this bias. We have followed the recipe given in Ref. [10]. An example of the effect of this correction is found in Fig. 1 (for the greatest lattice size simulated and $p = 0.9$, the same applies to other dilutions and lattice sizes): a great bias affects the non corrected numerical data and it is clear the importance to take into account this effect. In addition, it is clear that the recipe of Ref. [10] is working perfectly for $N_m = 100$, which is the number of measures per sample we have performed in this work. Therefore, we are very confident that all the data presented in this paper, processing with the recipe of reference [10] are not biased due to the reweighting technique.

On the other hand, we have tried to use the solution obtained in Ref. [15], where each sample is splitted in four parts, but the results were bad, this is due to the

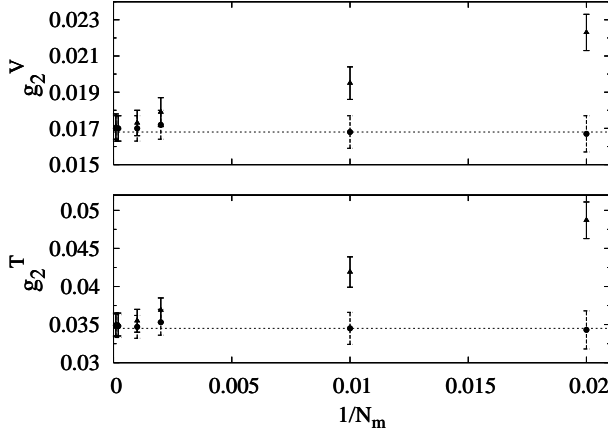


FIG. 1: The g_2 cumulant in both channels for $L = 64$, $p = 0.9$ with 1000 samples, $\beta_{\text{simulation}} = 0.79112$, reweighted at $\beta = 0.79082$ as a function of $1/N_m$, being N_m the number of measures in each sample. We report data with $N_m = 50; 100; 500; 1000; 5000; 10000$. The data without the bias correction proposed in Ref. [10] are marked with triangles while the corrected ones are marked with circles. We also mark with the dotted lines the election used in this work (which corresponds to $N_m = 100$). Notice the importance of the correction of the bias if one performs reweighting with the data.

small number of measures we take in each sample (10^2), which makes big differences between the averages in each quarter.

To compute errors in the averages we have used Jack-Knife methods, see Ref. [14]. We have defined 20 Jack-Knife blocks for the pure model in a unique sample and one block for each sample in the diluted ($p < 1$) models.

Calculated observables and critical exponents present sometimes, instead of a stable value, a monotonically decreasing one. For β , such an evolution with growing L is found, but it is clearly weaker than for β_c . In these cases an infinite volume extrapolation is called for. If hyperscaling holds, we expect finite-volume scaling corrections proportional to L^{-1} . This issue will be addressed in the next subsection.

B. The scaling exponent ν

As can be seen in Tables from IV to XI, allocated in the appendix A, specially for the thermal exponents and the cumulants (g_4 and g_2), there are evident finite volume effects so we have to use the equation:

$$\frac{x_0}{L} = \frac{x_0}{(L; 2L)} + \frac{\nu}{L}; \quad (22)$$

which is a consequence of scale-hypothesis, first derived in Ref. [16]. Consequently, choosing a good value for ν is a primordial question.

Exact results and RG calculations tell us that the disorder, being irrelevant in this model, induce scaling corrections with an exponent $\nu = -0.188$ (in L) [17]. In addition to this new scaling correction one must have the one of the pure model, which is related to the coupling of the $(\phi^2)^2$ term in the Ginzburg-Landau theory. This exponent is assumed to be 0.8 [18, 19] (for the pure model). Hence, the leading one is the exponent induced by the disorder. We will try to check this scenario by computing the "leading" correction to the scaling exponent from the numerical data.

First of all, we have tried to estimate ν just by considering it as another tunable parameter in Eq. (22) applied to some physical quantities. In these tests, as first approximation, we disregarded the possible correlations between the data for different L values, the results can be seen in Table I. If we perform a weighted average with this results we obtain $\nu = 1.07(9)$ for the pure model and $\nu = 0.92(9)$, $\nu = 0.81(7)$ and $\nu = 0.88(4)$ for the diluted model with $p = 0.9; 0.7$ and 0.5 respectively, in very good agreement with the value from the references given before. However, we think this method is not very confident because of the variability of the results from a quantity to another as shown in the Table I.

O	$\nu_{p=1.0}$	$\nu_{p=0.9}$	$\nu_{p=0.7}$	$\nu_{p=0.5}$
ν	1.45(52)			
M_ν	1.62(80)			
τ			1.2(1.1)	0.68(46)
M_τ				0.73(46)
g_4^v				
g_4^v	2.30(61)			0.62(47)
g_4^T				
g_4^T	2.12(52)	1.76(60)	1.09(40)	1.34(27)
$\nu=L$	1.08(21)	1.21(31)	0.61(12)	0.45(10)
$\tau=L$			1.55(76)	1.64(17)
g_4^v	0.85(14)	2.00(61)	1.21(15)	1.19(13)
g_4^T	1.06(14)		1.35(33)	1.41(42)
g_2^v		0.81(16)	0.89(9)	0.94(7)
g_2^T			0.63(12)	0.72(10)
ν_{weighted}	1.07(9)	0.92(9)	0.81(7)	0.88(4)

TABLE I: ν values from the $L \rightarrow 1$ extrapolations of some quantities. In the last row can be seen the weighted average of each column. We disregarded data with error bars bigger than the 100% of the values themselves. Those disregarded data are showed in the table as |.

Another approach, following Ref. [20], is to study the crossing points of scaling functions (as $\nu=L$ and g_4) measured in pairs of lattices with sizes L and $2L$. The deviation of these crossing point from the infinite volume critical coupling will behave as:

$$(L; sL) - (L; sL) = c(1) / \frac{1}{s^{\frac{1}{\nu}} - 1} L^{-\frac{1}{\nu}}; \quad (23)$$

With this method we need an additional estimate for the thermalexponent, we have used, following [11], the value $\beta = 0.7113(11)$ for the pure model (notice the really small error in β , so we will discard it in the following, see the comment at the end of this section), which is also a valid value for the diluted models, because of the validity of the Harris Criterion and as can be checked with the data in the Appendix A. Again we fixed $s = 2$. In this approach, we only use the crossing points in the vectorial channel because they are cleaner.

Extrapolating this crossing points using Eq.(23), we can plot the minimum of the χ^2 of the fit as a function of β obtaining the upper part of Fig. 2 and the whole Fig 3. To carry out this extrapolations we have to realize that the measures of the crossing points are correlated by pairs, so we have to use the χ^2 definition that include the whole selfcovariance matrix:

$$\chi^2_x = \sum_{l=1}^N \sum_{m=1}^N (x_{l1} - t)(\text{cov}^{-1})_{lm} (x_{m1} - t); \quad (24)$$

being N the number of crossing points, it is to say, the number of simulated L values minus two, x_{l1} is the obtained value for the observable x ($V=L$ or g_4^V), at the crossing point for L_1 and $2L_1$, and t is the fitted value to the form of Eq. (23) for L_1 . In addition:

$$(\text{cov})_{lm} = \langle x_{m1} x_{l1} \rangle - \langle x_{m1} \rangle \langle x_{l1} \rangle \quad (25)$$

can be also be deduced in terms of Jack-Knife blocks, see Ref. [14], as:

$$(\text{cov})_{lm} = \frac{N_b - 1}{N_b} \sum_{i=1}^{N_b} (x_{l1i}^{JK} - \langle x_{l1} \rangle) (x_{m1i}^{JK} - \langle x_{m1} \rangle); \quad (26)$$

where N_b is the number of Jack-Knife blocks, x_{l1i}^{JK} are block variables, where the first subindex runs over L values while the second one over $J-K$ blocks, and $\langle x_{l1} \rangle$ is the average between all block variables given $L = L_1$.

Also, following Ref. [20], we can do a joined fit in β of the crossing points of $V=L$ and g_4^V by defining:

$$\chi^2_{\text{joined}} = \chi^2_{V=L} + \chi^2_{g_4^V} \quad (27)$$

using Eq. (24) to calculate each one of the latter terms and searching for the minimum of χ^2_{joined} . We can obtain the error in β searching for the point β_1 in which $\chi^2_{\text{joined}}(\beta_1) = \chi^2_{\text{joined}}(\beta_{\text{min}}) + 1$, so the error is $\beta = \beta_{\text{min}} \pm \beta_1 - \beta_{\text{min}}$. The results for this joined fits are shown in the upper part of Fig. 2 and in the whole Fig. 3. We end with this method the values:

$$\beta = 0.96(15);$$

for the pure model and:

$$\beta = 2.29(70); 0.84(17); 0.64(13),$$

for the diluted models with $p = 0.9; 0.7$ and 0.5 respectively, in agreement with the value obtained in the pure model [8, 11, 18, 19], except in the $p = 0.9$ case, in which the value is far away two standard deviations from $\beta = 0.8$ [18, 19]. One possibility is that we are computing the leading correction to scaling exponent but with a large error. Another possibility is that in the $p = 0.9$ model the coefficients of the leading correction (from the numerical point of view) to the scaling vanishes or are very small. This result and the change in the slope of the g_4 data for $p < 1$ respect to the $p = 1$ ones, as can be seen in Table II, are evidences of the possible improved action found for $p = 0.9$, see Ref. [15], therefore the β exponent we are measuring in this case could correspond to the third irrelevant operator, instead of the second one (remember that following RG the first one is $\beta = 0.188$).

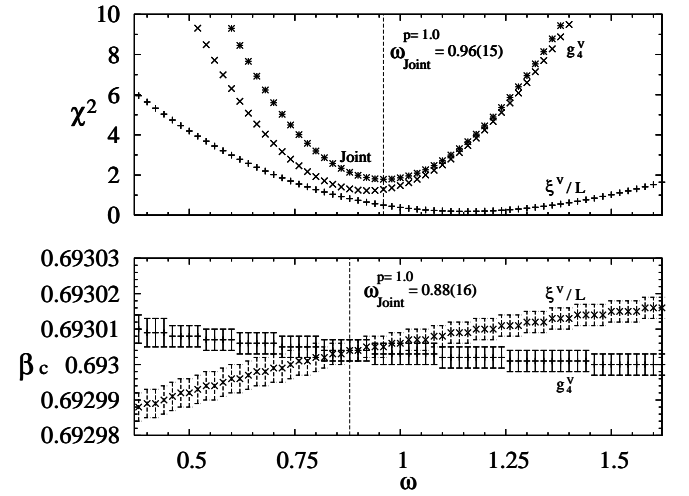


FIG. 2: Upper part: χ^2 as a function of β deduced from the fits to L^{-1} , Eq. (23), for the crossing point of $V=L$ and g_4 for the $(L, 2L)$ pair for the pure model. Also is shown the joined χ^2 . Lower part: extrapolated $\beta_c(1)$ as a β function, the point where both observables give the same extrapolated value is marked with the dotted line.

In addition, as Ref. [20] also did, we could estimate the correct value for β as the one producing the same $\beta_c(1)$ value for $V=L$ and g_4 , as can be seen in the lower part of Fig. 2, marked with the dotted line in $\beta = 0.88$. This approach only works for the pure model in which such a point is found, with another p value the $\beta_c(1)$ estimates from $V=L$ and g_4 do not cross each other.

In conclusion, we have shown that our data (both for the pure and diluted model) are fully compatible with the value $\beta = 0.80(1)$, obtained previously both numerically and analytically for the pure model [21]. In addition, since the error bars in β are really small (one per cent of error) we have discarded the uncertainty in β in the analysis presented in this paper, the error bars in the extrapolated quantities are much bigger than the uncertainty caused by the error bars in β : so we have fixed $\beta = 0.80$. The extrapolations (Tables III to X III) and

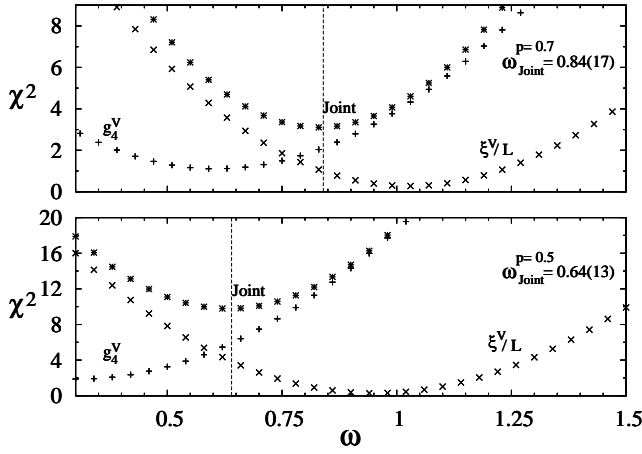


FIG. 3: Upper part: χ^2 as a function of ω for the diluted ($p = 0.7$) model. Also is shown the joined χ^2 . Lower part: χ^2 as a function of ω for the diluted ($p = 0.5$) model.

Figures (3 to 8) shown in the rest of the paper are obtained using this value of ω .

Finally, it is interesting to note that we have seen in the analysis presented in this subsection no traces of the leading correction to the scaling exponent even for the strongest dilution we have simulated, which should be $\omega = 0.188$. One can explain this fact assuming that the amplitudes of this scaling correction exponent are really small, so we are seeing the next to the leading scaling correction.

C. Numerical Results about Self-Averaging

Once that we have checked that the value $\omega = 0.80$ describe the corrections to the scaling in the pure and diluted model we can try to extrapolate the values of the two g_2 to infinite volume.

Numerical results for g_2 and g_4 in both channels are shown in Table II both for pure (only g_4) and diluted models.

First of all, we will try to check the non zero g_2 scenario with the correction to the scaling exponent fixed to that obtained in the previous section.

We have found that it is possible to extrapolate using the form of Eq. (22) (performing a joint fit [22]) the values of g_2 to a value (depending only on the channel), which is independent to the dilution, and near the analytical prediction of reference [3]. However, simulations (with a small number of samples), at dilutions $p = 0.95$ and $p = 0.97$ do not follow the scaling found for $p = 0.90$ (see Table III). Hence, our numerical data do not support the scenario $g_2 \neq 0$, see Figs. 4 and 5. Notice, see also Table III, that all the values for these two lowest dilutions are smaller than the extrapolated point and they are decreasing (for both channels and taking into account the error bars).

p	L	g_2^V	g_2^T	g_4^V	g_4^T
1.0	8	0	0	0.62243 (4)	0.5216 (1)
	12	0	0	0.62172 (5)	0.5189 (2)
	16	0	0	0.62152 (6)	0.5181 (2)
	24	0	0	0.62100 (5)	0.5166 (2)
	32	0	0	0.62092 (3)	0.5162 (1)
	48	0	0	0.62066 (5)	0.5156 (2)
0.9	8	0.0327 (4)	0.0576 (7)	0.6151 (2)	0.5102 (3)
	12	0.0273 (3)	0.0518 (6)	0.6163 (1)	0.5104 (3)
	16	0.0253 (3)	0.0499 (6)	0.6166 (1)	0.5100 (3)
	24	0.0226 (3)	0.0453 (6)	0.6168 (1)	0.5098 (3)
	32	0.0208 (2)	0.0421 (5)	0.6171 (1)	0.5100 (3)
0.7	8	0.0780 (8)	0.1406 (16)	0.6061 (3)	0.4994 (6)
	12	0.0610 (6)	0.1177 (13)	0.6108 (2)	0.5039 (5)
	16	0.0512 (5)	0.1009 (11)	0.6131 (2)	0.5064 (4)
	24	0.0423 (4)	0.0868 (10)	0.6150 (2)	0.5077 (4)
	32	0.0371 (4)	0.0770 (9)	0.6160 (2)	0.5089 (4)
0.5	8	0.1130 (11)	0.2061 (24)	0.6006 (4)	0.4999 (8)
	12	0.0834 (8)	0.1600 (18)	0.6072 (3)	0.5047 (6)
	16	0.0702 (7)	0.1395 (16)	0.6107 (3)	0.5070 (6)
	24	0.0553 (6)	0.1138 (13)	0.6138 (2)	0.5085 (5)
	32	0.0474 (5)	0.0980 (11)	0.6151 (2)	0.5095 (4)

TABLE II: Cumulants for the O(3) model. In the first column is represented the spin density p . All the cumulants are calculated in the crossing points of $\omega = L$ for L and $2L$. The averages have been computing using 10^4 samples (except in the $p = 1$) case.

Secondly, we will check the $g_2 = 0$ scenario. To do this, we extrapolate g_2 using the form proposed in Ref. [2] ($g_2 \propto L^{-\omega}$) but also including the term L^{-1} :

$$g_2 = aL^{-\omega} + bL^{-1} \quad (28)$$

We obtain the fits shown in Figs. 6 and 7 for both channels. The χ^2 of these all fits are really good, hence, we have obtain strong evidence supporting this $g_2 = 0$ scenario. Notice that the introduction of the scaling correction has had paramount importance in order to obtain very good χ^2 in all the fits. The numerical data, for the lattice size simulated, does not follow the one term dependence $g_2 \propto L^{-\omega}$.

V. CONCLUSIONS

We have studied the critical properties of the Heisenberg diluted model for different values of the dilution using the quotient method. Our main aim was to check the self-averaging properties of the susceptibility.

We have studied in a great detail the corrections to the scaling in the diluted Heisenberg model. We have obtained that the numerical data follow the next to the leading correction to the scaling exponent instead the

p	L	g_2^V	g_2^T	g_4^V	g_4^T
0.97	8	0.0108 (6)	0.0181 (13)	0.6201 (4)	0.5187 (10)
	12	0.0102 (6)	0.0189 (14)	0.6195 (4)	0.5164 (10)
	16	0.0084 (6)	0.0158 (12)	0.6201 (4)	0.5159 (10)
	24	0.0072 (5)	0.0146 (11)	0.6206 (4)	0.5162 (9)
	32	0.0074 (5)	0.0152 (12)	0.6206 (4)	0.5152 (10)
0.95	8	0.0179 (10)	0.0290 (18)	0.6180 (5)	0.5158 (11)
	12	0.0167 (9)	0.0329 (20)	0.6182 (5)	0.5116 (12)
	16	0.0150 (9)	0.0286 (18)	0.6181 (5)	0.5129 (11)
	24	0.0117 (7)	0.0228 (14)	0.6186 (4)	0.5135 (11)
	32	0.0118 (7)	0.0251 (17)	0.6193 (4)	0.5140 (10)

TABLE III: Cumulants for the O(3) model with high p values. All the cumulants are computed averaging only 10^3 samples.

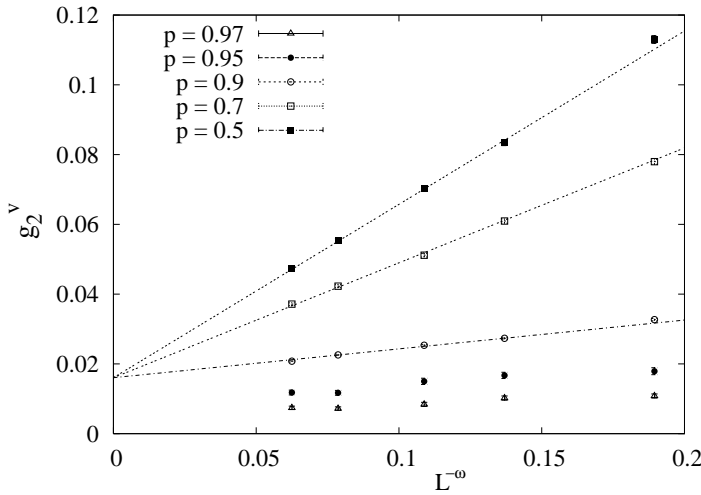


FIG. 4: Joint extrapolation to $L \rightarrow \infty$ for the g_2 cumulant of the vectorial susceptibility. Extrapolations are carried out by choosing a common value for the first term of Eq. (22) for all dilutions and by minimizing the joined χ^2 . We have disregarded the data with $L = 8$ to obtain a good value of the χ^2 .

leading one. We will show in the appendix all the critical exponents and cumulants using this next to the leading exponent, also we report that the result of this analysis is fully compatible with the RG predictions and the Harris-Criterion: our exponents and cumulants are compatibles with that of the pure model and independent of the dilution with a high degree of precision.

In addition, we have shown that we obtain non universal quantities if we assume $\omega = 0$ as the main scaling correction even if we add the ω correction to the scaling exponent (see the appendix), using two correction to scaling exponents in the analysis.

Finally, we have shown strong evidence for a zero g_2 cumulant, both in vector and tensor channels, in the thermodynamic limit at criticality, contrasting with some analytical predictions [3], and in agreement with the ones

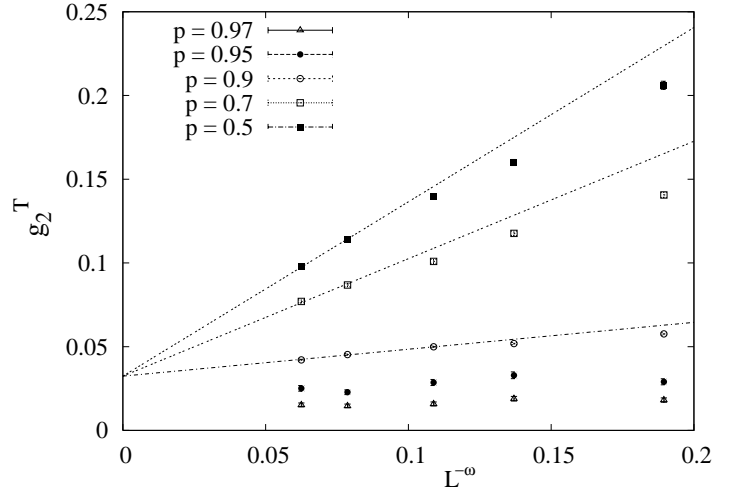


FIG. 5: Joint extrapolation to $L \rightarrow \infty$ for the g_2 cumulant of the tensorial susceptibility, to the form of Eq. (22).

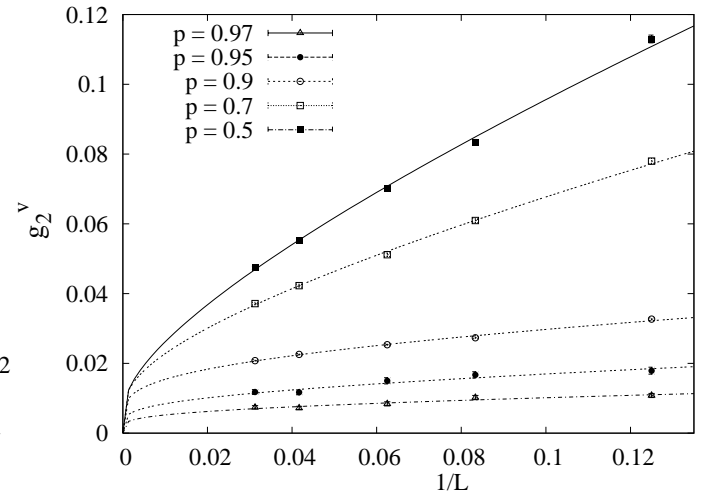


FIG. 6: Extrapolation to $L \rightarrow \infty$ for the g_2 cumulant of the vectorial susceptibility. The fitting function is in this case of the form $g_2 = aL^{-\omega} + bL^{-1}$.

obtained in Ref. [2]. The introduction of scaling corrections in the analysis has become crucial to obtain the $g_2 = 0$ scenario. In addition, simulations of samples with lower dilution have helped to discard the $g_2 \neq 0$ scenario.

Acknowledgments

This research has been supported by the Ministerio de Educaci3n y Ciencia (Spain) through grant No. FIS2004-01399 (partially financed by FEDER funds), through grant No. BFM 2003-C08532 and by the European Community's Human Potential Programme under contract HPRN-CT-2002-00307. The computations have been carried out using the resources of the BIFI (Instituto de Biocomputaci3n y F3sica de Sistemas Complejos) placed

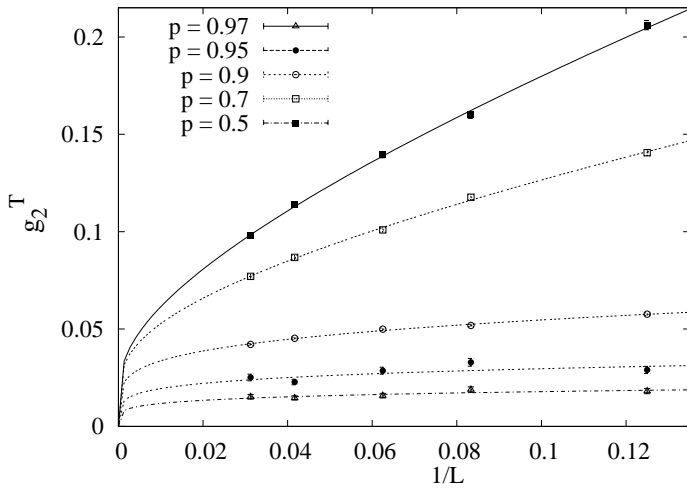


FIG. 7: Extrapolation to $L \rightarrow 1$ for the g_2 cumulant of the tensorial susceptibility to the form $g_2 = aL^\alpha + bL^\beta$.

in Zaragoza, Spain. We thank A. Pelissetto and E. Vicari for pointing us the relevance of the scaling corrections in the analysis of the $g_2 = 0$ scenario. We also have to thank L. A. Fernandez, V. Martı́n-Mayor, and E. Konutcheva for interesting discussions.

APPENDIX A: CRITICAL EXPONENTS AND CUMULANTS

In this appendix we will check the consistency of the ν exponent computed in the text by means of the computation of critical exponents and cumulants. In addition, we will check if these sets of exponents are Universal or not by comparing different dilutions with the pure model. We will use in this analysis the data from $p = 0.9; 0.7$ and 0.5 (we have simulated in these values of the dilution 10^4 samples).

Eq. (17) applied to the operators ϕ , ϕ_{g_4} , M and χ , yields respectively the critical exponents $1 + \nu$, $1 - \nu$, $(d - 2 + \nu)/2$ and $2 - \nu$. The numerical results are shown in Tables IV and V for the pure model, Tables VI and VII for $p = 0.9$, Tables VIII and IX for $p = 0.7$ and Tables X and XI for $p = 0.5$. We have also carried out a joined extrapolation for every p values by fixing the same value of the extrapolated exponent (first term in Eq. (22)) for every p value and then minimizing the joined χ^2 . Some of these fits are shown in figures 8 to 11 and the compared results can be seen in Tables XII and XIII.

The joined extrapolation of the Binder cumulant g_4 is shown in Table XIV and the agreement of our results with the ones obtained in Refs. [1] (numerical for the pure model) and [3] (analytical) is really very good. We obtain also complete agreement with previous numerical estimates of the pure model critical exponents, see Ref. [1].

We obtain non universal critical exponents and cumu-

lants if instead $\nu = 0.8$ we use $\nu = \nu_{\text{pure}}$ as the correction to scaling exponent. In addition, the dilution dependent exponents and cumulants are clearly different of the pure ones. Furthermore, this scenario does not change if we fit the data using both $\nu = \nu_{\text{pure}}$ and $\nu = 0.8$.

L	ν			
	ν	M	τ	M_τ
8	0.0301 (7)	0.0319 (8)	1.4301 (12)	1.4343 (13)
12	0.0339 (7)	0.0353 (8)	1.4324 (11)	1.4352 (12)
16	0.0348 (7)	0.0358 (8)	1.4310 (11)	1.4335 (12)
24	0.0361 (6)	0.0367 (7)	1.4293 (9)	1.4307 (10)
32	0.0369 (7)	0.0374 (7)	1.4289 (11)	1.4300 (12)
48	0.0373 (6)	0.0378 (7)	1.4271 (9)	1.4280 (10)
$L \rightarrow 1$	0.0391 (9)	0.0390 (10)	1.4250 (13)	1.4249 (15)
χ^2/dof	0.138/3	0.354/3	1.047/3	1.952/3
prob	0.987	0.950	0.790	0.582

TABLE IV: Magnetic exponents for the pure O(3) model. The last three rows correspond to the $L \rightarrow 1$ extrapolation (disregarding data with $L = 8$)

L	ν			
	$\nu_{g_4^V}$	ν^V	$\nu_{g_4^T}$	ν^T
8	0.7016 (30)	0.7217 (13)	0.6846 (41)	0.7306 (14)
12	0.7033 (32)	0.7162 (14)	0.6931 (49)	0.7188 (13)
16	0.7028 (35)	0.7123 (16)	0.6830 (56)	0.7118 (17)
24	0.7061 (37)	0.7123 (17)	0.6908 (47)	0.7112 (18)
32	0.7081 (35)	0.7121 (19)	0.7022 (61)	0.7116 (23)
48	0.7101 (41)	0.7118 (19)	0.7125 (61)	0.7085 (21)
$L \rightarrow 1$	0.7109 (38)	0.7071 (19)	0.7082 (51)	0.7071 (35)
χ^2/dof	0.667/4	4.104/4	7.039/4	0.565/2
prob	0.954	0.392	0.134	0.754

TABLE V: Thermal critical exponents for the pure O(3) model. In the last column we have disregarded data with $L < 16$.

L			T	
			τ	M_τ
8	0.0346 (26)	0.0345 (28)	1.4154 (36)	1.4176 (37)
12	0.0360 (24)	0.0360 (26)	1.4195 (34)	1.4207 (36)
16	0.0371 (23)	0.0374 (25)	1.4207 (34)	1.4218 (35)
24	0.0373 (22)	0.0375 (24)	1.4204 (32)	1.4221 (34)
32	0.0383 (21)	0.0383 (23)	1.4219 (31)	1.4227 (33)
L ! 1	0.0397 (29)	0.0399 (31)	1.4245 (41)	1.4252 (43)
$^2=\text{dof}$	0.292/3	0.124/3	0.544/3	0.137/3
prob	0.962	0.989	0.909	0.987

TABLE V I: M agnetic exponents for the diluted O (3) m odel with $p= 0.9$. E xtrapolations are carried out w ithout disregarding data.

L			T	
			τ	M_τ
8	0.7888 (69)	0.7881 (31)	0.8256 (143)	0.8422 (42)
12	0.7810 (74)	0.7806 (33)	0.8078 (140)	0.8067 (41)
16	0.7633 (70)	0.7760 (35)	0.7739 (131)	0.7897 (43)
24	0.7491 (66)	0.7628 (37)	0.7719 (146)	0.7792 (47)
32	0.7400 (67)	0.7521 (42)	0.7656 (178)	0.7627 (56)
L ! 1	0.7206 (88)	0.723 (10)	0.729 (19)	0.7255 (61)
$^2=\text{dof}$	2.313/3	0.281/1	1.314/3	1.965/3
prob	0.510	0.596	0.726	0.580

TABLE IX : Therm al exponents for the diluted O (3) m odel with $p= 0.7$. In the second column the τ is obtained disregarding data with $L < 16$.

L			T	
			τ	M_τ
8	0.7319 (49)	0.7443 (24)	0.7128 (83)	0.7709 (29)
12	0.7381 (53)	0.7411 (25)	0.7267 (86)	0.7514 (29)
16	0.7430 (55)	0.7381 (26)	0.7536 (99)	0.7426 (31)
24	0.7384 (57)	0.7368 (28)	0.7337 (95)	0.7395 (32)
32	0.7398 (54)	0.7365 (29)	0.7241 (97)	0.7345 (33)
L ! 1	0.734 (15)	0.7318 (33)	0.728 (17)	0.7152 (39)
$^2=\text{dof}$	0.134/1	0.168/3	5.468/2	3.156/3
prob	0.714	0.983	0.065	0.368

TABLE V II: Therm al exponents for the diluted O (3) m odel with $p= 0.9$. In the rst and third columns we obtain bad results because not m onotonally-decreasing series.

L			T	
			τ	M_τ
8	0.0505 (45)	0.0461 (48)	1.3435 (61)	1.3431 (62)
12	0.0448 (39)	0.0439 (42)	1.3684 (54)	1.3702 (56)
16	0.0421 (36)	0.0417 (39)	1.3877 (51)	1.3896 (52)
24	0.0396 (32)	0.0406 (35)	1.4033 (46)	1.4053 (48)
32	0.0399 (30)	0.0414 (32)	1.4126 (43)	1.4152 (45)
L ! 1	0.0346 (60)	0.0378 (46)	1.446 (12)	1.449 (12)
$^2=\text{dof}$	2.225/2	2.191/3	0.119/1	0.327/1
prob	0.329	0.534	0.730	0.568

TABLE X : M agnetic exponents for the diluted O (3) m odel with $p= 0.5$. In the third and fourth columns we have only used data with $L > 12$.

L			T	
			τ	M_τ
8	0.0436 (38)	0.0412 (41)	1.3882 (52)	1.3879 (53)
12	0.0411 (34)	0.0401 (36)	1.4005 (48)	1.4007 (49)
16	0.0392 (31)	0.0392 (34)	1.4061 (45)	1.4073 (46)
24	0.0383 (29)	0.0386 (31)	1.4131 (41)	1.4136 (43)
32	0.0382 (27)	0.0389 (29)	1.4142 (40)	1.4149 (41)
L ! 1	0.0343 (57)	0.0370 (58)	1.4299 (72)	1.4318 (76)
$^2=\text{dof}$	0.232/3	0.059/3	0.472/3	0.567/3
prob	0.972	0.996	0.925	0.904

TABLE V III: M agnetic exponents for the diluted O (3) m odel with $p= 0.7$. E xtrapolations are carried out w ithout disregarding data.

L			T	
			τ	M_τ
8	0.8102 (91)	0.8357 (46)	0.9180 (241)	0.9540 (72)
12	0.8042 (90)	0.8322 (50)	0.8880 (248)	0.8866 (71)
16	0.7764 (89)	0.7862 (48)	0.8449 (242)	0.8136 (64)
24	0.7702 (93)	0.7778 (52)	0.8311 (234)	0.7952 (66)
32	0.7562 (91)	0.7779 (56)	0.7812 (220)	0.7833 (70)
L ! 1	0.720 (16)	0.764 (14)	0.735 (28)	0.744 (17)
$^2=\text{dof}$	1.149/2	0.208/1	1.565/3	0.025/1
prob	0.563	0.649	0.667	0.874

TABLE X I: Therm al exponents for the diluted O (3) m odel with $p= 0.5$. In the rst column we have only used data with $L > 8$ while in the second and fourth ones we have only use data with $L > 12$.

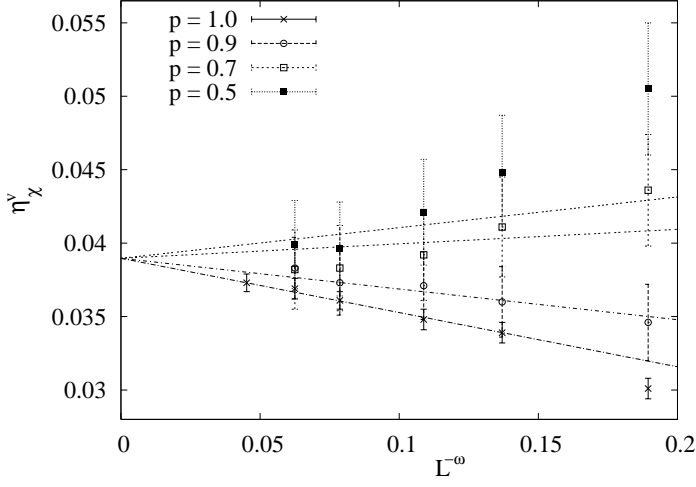


FIG. 8: Joined extrapolation to $L \rightarrow 1$ for the exponent deduced from the vectorial susceptibility (χ^v). Extrapolations are carried out by choosing a common value for the first term of Eq. (22) for all dilutions, and by minimizing the joined χ^2 .

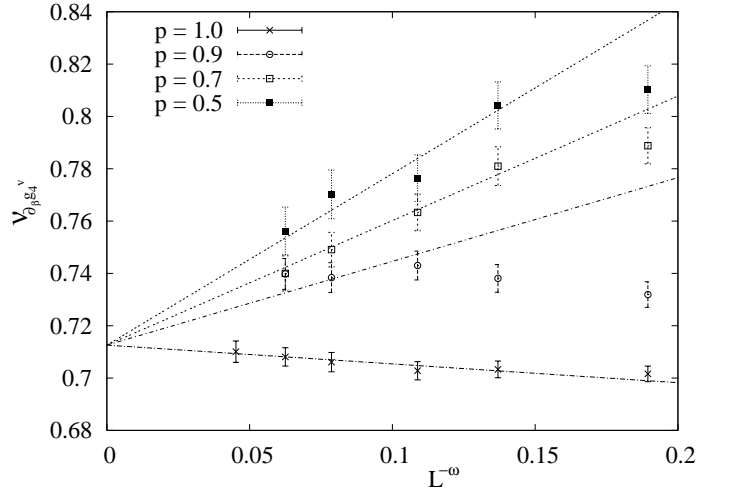


FIG. 10: Joined extrapolation with all p values to $L \rightarrow 1$ for the exponent deduced from the g_4^v .

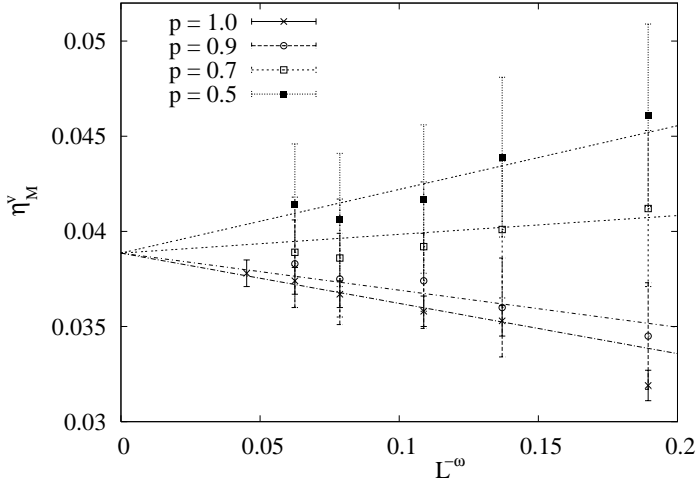


FIG. 9: Joined extrapolation with all p values to $L \rightarrow 1$ for the exponent deduced from the vectorial magnetization (M^v).

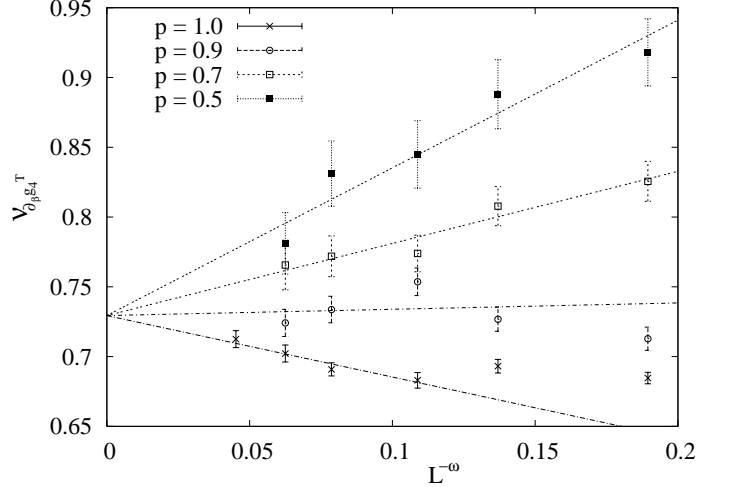


FIG. 11: Joined extrapolation to $L \rightarrow 1$ for the exponent deduced from the g_4^T .

	T			
		M	T	M _T
Our results	0.0390 (9)	0.0389 (10)	1.4251 (13)	1.4251 (14)
χ^2/dof	6.675/12	5.104/15	9.151/10	13.931/11
prob	0.878	0.991	0.518	0.237
Ref: [11]	0.0378 (6)			

TABLE XII: Joined extrapolation with all p values for the magnetic exponent compared with the results from Ref. [11]. The first three rows correspond to our $L \rightarrow 1$ extrapolation, being prob the probability to find a larger value for the χ^2 of the fit (it is a measure of the goodness of the fit) and dof : the number of degrees of freedom (the total number of data minus the total number of adjustable parameters in the fitting function).

	$@ g_4^V$	$@^V$	$@ g_4^T$	$@^T$
Our results	0.7126 (46)	0.7129 (31)	0.7294 (81)	0.7089 (32)
χ^2/dof	4.831/11	6.606/6	9.009/13	9.609/7
prob	0.939	0.359	0.772	0.212
Ref: [11]	0.7113 (11)			

TABLE X III: Joined extrapolation with all p values for the thermalexponent compared with the results from Ref. [11].

	g_4^V	g_4^T
Our results	0.62018 (6)	0.51366 (19)
χ^2/dof	10.324/9	5.980/10
prob	0.325	0.817
Ref: [11]	0.6202 (1)	
Ref: [3]	0.625783	

TABLE X IV :Joined extrapolation to $L \rightarrow 1$ with all p values for the Binder cumulant, g_4 , defined in Eq. (11), compared with results from Refs.[11] and [3].

-
- [1] A. B. Harris, J. Phys. C 7, 1671 (1974).
- [2] A. Aharony and A. B. Harris, Phys. Rev. Lett. 77, 3700 (1996).
- [3] H. Chatani, E. Korutcheva and N. S. Tonchev, Phys. Rev. E 65, 026129 (2002).
- [4] A. Aharony and A. B. Harris, S. Wiseman Phys. Rev. Lett. 81, 252 (1998).
- [5] S. Wiseman, E. Domany, Phys. Rev. E 58, 2938 (1998).
- [6] C. Deroulers, A. P. Young, Phys. Rev. B 66, 014438 (2002).
- [7] G. Parisi, M. Picco and N. Sourlas, Europhys. Lett. 66, 465 (2004).
- [8] H. G. Ballesteros, L. A. Fernandez, V. Martin-Mayer, A. Munoz Sudupe, Phys. Lett. B 387, 125-131 (1996).
- [9] H. G. Ballesteros, L. A. Fernandez, V. Martin-Mayer, A. Munoz Sudupe, G. Parisi, J. J. Ruiz-Lorenzo, Phys. Lett. B 400, 346 (1997).
- [10] H. G. Ballesteros, L. A. Fernandez, V. Martin-Mayer, A. Munoz Sudupe, G. Parisi and J. J. Ruiz-Lorenzo, Nucl. Phys. B 512, 681-701 (1998).
- [11] M. Campostrini, M. Hasenbusch, A. Pelissetto, P. Rossi and E. Vicari, Phys. Rev. B 65, 144520 (2002).
- [12] E. Brezin and J. Zinn-Justin, Nucl. Phys. B 257 [FS14], 867 (1985).
- [13] F. Cooper, B. Freedman and D. Preston, Nucl. Phys. B 210, 210 (1982).
- [14] D. J. Amit and V. Martin-Mayor, Field Theory, The Renormalization Group and Critical Phenomena, World Scientific Publishing, 2005.
- [15] M. Hasenbusch, F. P. Toldin, A. Pelissetto and E. Vicari, J. Stat. Mech. P016, 702 (2007).
- [16] M. E. Fisher and M. N. Barber, Phys. Rev. Lett. 28, 1516 (1972).
- [17] A. Pelissetto and E. Vicari, Phys. Rep. 368, 549 (2002).
- [18] R. Guida and J. Zinn-Justin, J. Phys. A 31, 8103-8121 (1998) and references therein.
- [19] M. Hasenbusch, J. Phys. A 34, 8221 (2001).
- [20] H. G. Ballesteros, L. A. Fernandez, V. Martin-Mayer, A. Munoz Sudupe, G. Parisi and J. J. Ruiz-Lorenzo, Phys. Rev. B 58, 2740 (1998).
- [21] In more detail, the field theoretical approaches (both ϵ -dimension and ϵ -expansion) provide very accurate values for β : 0.782(13) and 0.794(18) (respectively) [18]. Recent numerical simulations bring us the values 0.775(13) and 0.799(13) [19] and 0.64(13) and 0.71(15) [8].
- [22] We have used to do all the data set which gives out the smallest χ^2 with the biggest number of degrees of freedom.